



BEACHMED-E
SOUS-PROJET 2.2

Characterization of nearshore hydro-meteorological conditions, analysis of littoral risks, behaviour of coastal defence structures and *Posidonia oceanica* dynamics
NAUSICAA

Frédéric Bouchette
Laboratoire Géosciences Montpellier, CNRS / Université Montpellier II
GEOSCIENCES-M (bouchette@dstu.univ-montp2.fr)

PHASE C INTERMEDIATE REPORT
Short version



MOTS-CLES

Mesure et modélisation hydrodynamique, Atlas, CSI, *Posidonia oceanica*

INTRODUCTION

Dans ce projet, on s'intéresse à la dynamique littorale et ses conséquences au travers des 4 problématiques scientifiques suivantes: 1. la caractérisation des climats de houle et des conditions hydrodynamiques et météorologiques, sur la base de mesures et de modélisations; 2. l'étude des phénomènes d'érosion et de surcôte de tempête en zone littorale; 3. l'étude des processus d'endommagement des ouvrages artificiels de protection en zone littorale et le développement de méthodes pour le suivi et la prédiction de leur comportement; 4. l'étude des processus d'interaction entre la houle et les biotopes marins (exemple des prairies de *Posidonia oceanica*). Ces questions sont traitées sur un certain nombre de chantiers répartis sur l'ensemble des régions d'origine des partenaires. L'ensemble des sites retenus concerne des littoraux à dominante sableuse, avec présence éventuelle de structures artificielles de protection du littoral et/ou de prairies de *Posidonia oceanica*. Le traitement de ces questions repose avant tout sur une bonne détermination de l'hydrodynamique côtière à littorale sur les zones étudiées. L'ensemble des travaux menés par les équipes de recherche a donc pour **dénominateur commun la modélisation numérique et la mesure in-situ des processus hydrodynamiques et hydrosédimentaires littoraux**. En outre, la méthodologie employée est commune à l'ensemble des partenaires et peut être résumée de la manière suivante: 1. Sélection de chantiers d'études cohérents pour les problématiques traitées et synthèse bibliographique des données hydrodynamiques et autres disponibles sur ces chantiers; 2. organisation et réalisation de campagnes de mesures hydrodynamiques à différentes échelles de temps et d'espace sur les chantiers retenus; 3. modélisation des processus hydrodynamiques, hydrosédimentaires et/ou hydrobiologiques validés et calibrés par les mesures d'archives et/ou acquises sur les chantiers retenus dans le cadre du projet; 4. Réalisation de produits spécifiques pour répondre aux différents problèmes traités: atlas hydrodynamique du littoral (érosion et surcôte), détermination de CSI (Coastal State Indicators), cartes de la dynamique des prairies de *Posidonia oceanica*, documents synthétiques.

La phase C du projet NAUSICAA (détaillée dans le dossier consolidé) est axée sur la généralisation des travaux de modélisation hydrodynamique et la réalisation des livrables finaux.

Ce document est une version synthétique et abrégée de la présentation du bilan intermédiaire de la phase C.

Dans ce document, on trouve:

- 1) un extrait d'Atlas Hydrodynamique reposant sur une charte graphique discutée avec les utilisateurs finaux de ce type de document. L'ébauche est proposée pour la partie Nord du Golfe du Lion, en France;
- 2) les résultats de modélisation sur le Lido de Dante et Igea Marina;
- 3) une présentation des résultats numériques obtenus en Mer Egée dans le cadre de la réalisation d'un Atlas hydrodynamique du Nord de la Mer Egée (Macédoine Thrace);
- 4) les résultats de modélisation visant à comprendre les relations entre la dynamique des herbiers de *Posidonia O.* et le forçage hydrodynamique.

Atlas hydrodynamique en Languedoc-Roussillon

Un atlas hydrodynamique est un outil amené à être manipulé par des utilisateurs finaux ayant besoin d'être guidés vers une interprétation juste et raisonnable de cartes résultants de mesures et de modélisations de l'hydrodynamique littorale. Pour répondre à cette exigence, la conception de l'Atlas Hydrodynamique comprend une phase de réflexion sur son apparence et sa structure. Un objectif essentiel de la phase B était de proposer une ébauche de ce que doit être la maquette finale de l'Atlas Hydrodynamique.

L'idée de fond est que l'Atlas en version papier est un document au format A3 en couleur. Lorsqu'il est ouvert, sur un ensemble de 2 pages A3 en regard l'une de l'autre, on trouve un ensemble de figures et d'informations textuelles qui correspondent à un forçage donné (conditions de vent et conditions de houle au large) sur un site donné. Ici, on montre un exemple de résultats de l'Atlas dans son état d'avancement actuel. L'exemple retenu pour cette version abrégée est le forçage de vent de Sud-Ouest sur l'ensemble du Golfe d'Aigues-Mortes (échelle pré-littorale, boîte Nord). Même si les modélisations de la propagation de la houle sont réalisées (voir par exemple document de présentation de la fin de PHASE B lors de la réunion de Bologne en Avril 2007), aucun résultat de couplage houle / courant n'a été représenté dans la mesure où ils sont tous en cours de validation. L'ensemble des résultats validés est disponible dans la version longue du rapport de phase B. Au 30 juin 2007, cet ensemble correspond à un peu moins de 400 cartes pour un total de plusieurs dizaines de Gb de données.

Sur les figures 1 et 2, on retrouve les deux pages A3 montrant les résultats pour l'exemple sélectionné.

Les résultats sont organisés de la manière suivante: 1) un bandeau supérieur reprenant les caractéristiques générales du cas étudié, 2) un texte commentaire sur la partie droite extrême guidant l'utilisateur dans l'interprétation des résultats reportés sur les différentes figures constituant le panneau, 3) deux cartouches, l'un rappelant la position du domaine modélisé à l'échelle du Golfe du Lion bien visible lorsqu'on effeuille l'atlas, l'autre (en bas) montrant la topobathymétrie et (à terme) de manière graphique le type de forçage appliqué pour le cas étudié, 4) un ensemble de 5 cartes, 2 coupes et 1 graphe représentant des grandeurs physiques, chaque figure étant nommée et systématiquement repérée par un code lettre qui est repris dans les explications données dans le texte.

On propose une description rapide des différentes figures sélectionnées:

Figure A: une représentation des courants de surface résultant du forçage courant. Ce forçage peut être un vent seul (comme c'est le cas dans les deux exemples ici), une houle au large seule, ou à la fois un vent et une houle. Dans le cas d'un vent seul, on a une représentation de la circulation décrite par les modèles traditionnels en océanographie. Dans le cas d'une forçage houle/courant, la circulation est la résultante du couplage complexe entre les deux forçages, comme décrit en phase A.

Figure B: une représentation des courants de fond résultant du forçage courant. Les remarques ci-dessus s'appliquent également.

Figure C: une représentation de la vitesse moyenne sur la verticale qui donne une indication du transport de masse d'eau (à ne pas confondre avec le transport sédimentaire).

Figure D: une représentation de la hauteur des vagues.

Figures E et F: des coupes verticales représentant le courant résultant du forçage. Le panneau final offrira un positionnement de ces coupes sur la figure représentant la topobathymétrie.

Figure G: une représentation de l'élévation de la surface libre résultant du forçage courant. Dans le cas d'un vent seul, on a donc une représentation du basculement du plan d'eau sous le cisaillement induit par le vent. Dans le cas de la houle, on a une représentation de la surcôte, et dans le cas d'un forçage combiné houle/vent, on a les deux.

Figure H: une représentation de l'élévation de la surface libre dans 5, 10 et 20 mètres d'eau.

Une version de l'atlas est prévue on-line, avec des représentations graphiques additionnelles: vitesses de Stokes, vitesse orbitale, vitesse de phase, vitesses dans la colonne d'eau (et non pas seulement à la surface et au fond).

1.13 Conditions de Marin du Sud-Est avec houle $H = 4m$, $T = 10s$ en provenance de l'Est : plateau interne central

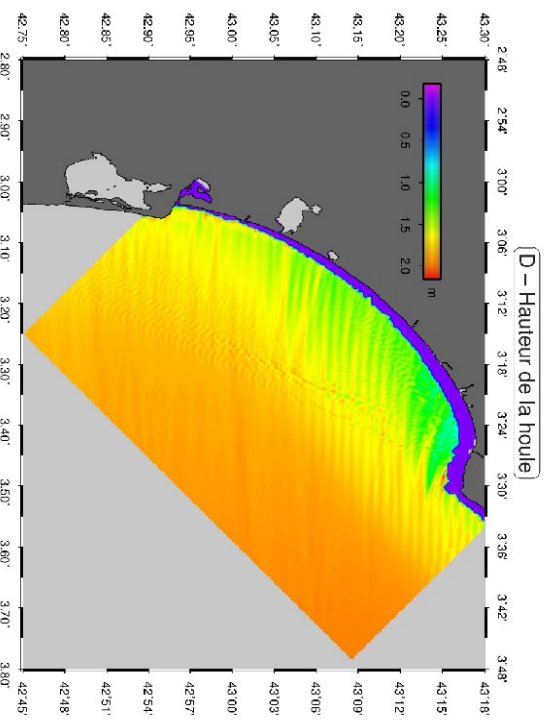
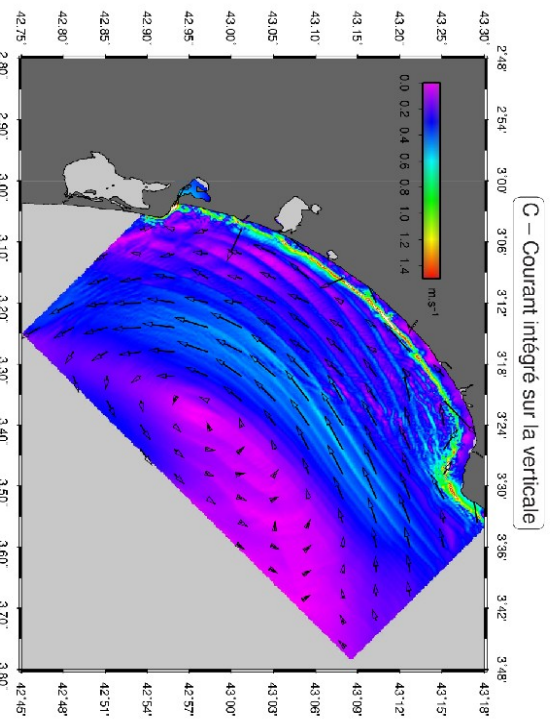
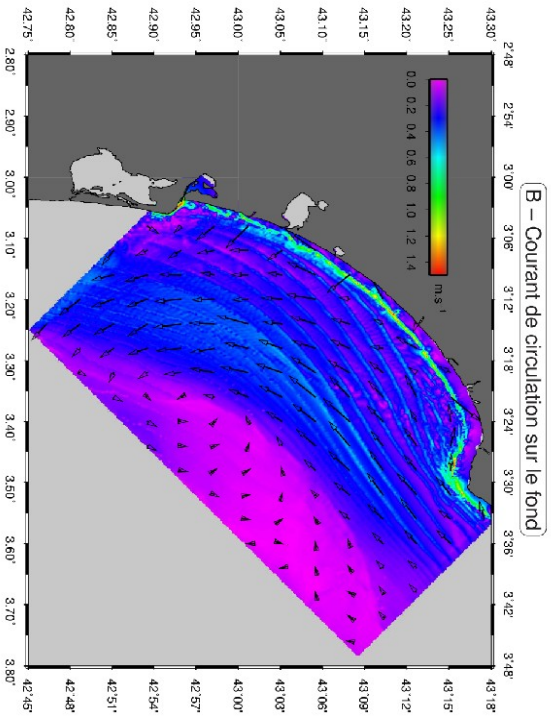
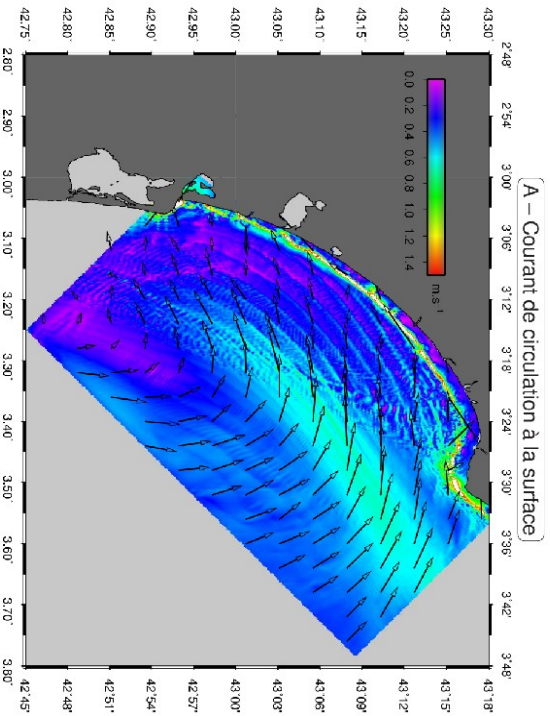
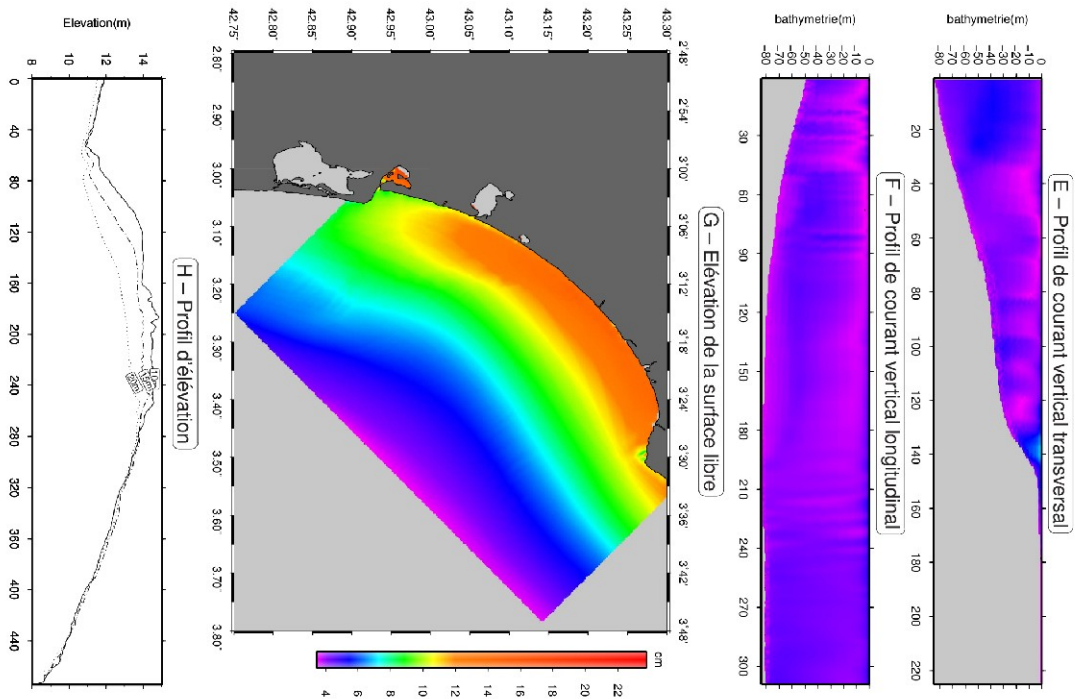
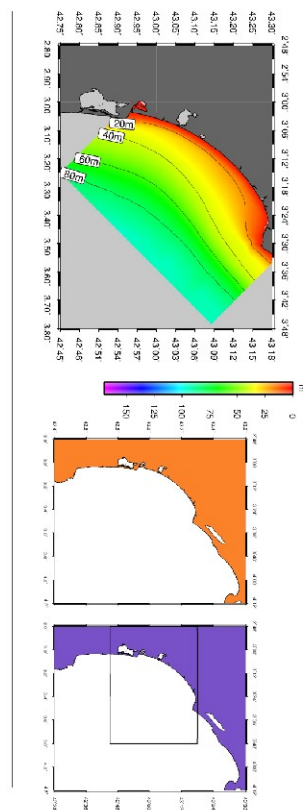


Figure 1: représentation à un format réduit du premier A3 du modèle d'atlas hydrodynamique pour le cas d'une houle d'Est sur la boîte pré-littorale Centre.



Conditions de Marin du Sud-Est avec houle $H = 2m$, $T = 8s$ en provenance du Sud-Est : plateau interne central



Contexte
 Descriptif
 Aspects numériques

Figure 2: représentation à un format réduit du second A3 du modèle d'atlas hydrodynamique pour le cas d'une houle d'Est sur la boîte pré-littorale Centre. La partie laissée ici en blanc contient des explications sur l'hydrodynamique en français ou en anglais.

Les scénarios calculés, traités et finalisés au moment de la rédaction de ce rapport sont les suivants (sachant que l'atlas va continuer à s'enrichir dans les mois et les années à venir):

Conditions de Mistral de Nord-Est à 55 km.h⁻¹ : plateau interne du Golfe d'Aigues-Mortes

Conditions de Marin du Sud-Est à 55 km.h⁻¹ : plateau interne du Golfe d'Aigues-Mortes

Conditions de vent de Sud-Ouest à 55 km.h⁻¹ : plateau interne du Golfe d'Aigues-Mortes

Conditions de Tramontane du Nord-Ouest à 55 km.h⁻¹ : plateau interne du Golfe d'Aigues-Mortes

Conditions de houle seule H = 2m, T = 8s en provenance de l'Est : plateau interne central

Conditions de houle seule H = 2m, T = 8s en provenance du Sud-Est : plateau interne central

Conditions de houle seule H = 4m, T = 10s en provenance de l'Est : plateau interne central

Conditions de houle seule H = 4m, T = 10s en provenance du Sud-Est : plateau interne central

Conditions de houle seule H = 6m, T = 12s en provenance de l'Est : plateau interne central

Conditions de houle seule H = 6m, T = 12s en provenance du Sud-Est : plateau interne central

Conditions de Marin du Sud-Est avec houle H = 2m, T = 8s en provenance de l'Est : plateau interne central

Conditions de Marin du Sud-Est avec houle H = 2m, T = 8s en provenance du Sud-Est : plateau interne central

Conditions de Marin du Sud-Est avec houle H = 4m, T = 10s en provenance de l'Est : plateau interne central

Conditions de Marin du Sud-Est avec houle H = 4m, T = 10s en provenance du Sud-Est : plateau interne central

Conditions de Marin du Sud-Est avec houle H = 6m, T = 12s en provenance du Sud-Est : plateau interne central

Conditions de Marin du Sud-Est à 55 km.h⁻¹ : plateau interne central

Conditions de Tramontane du Nord-Ouest à 55 km.h⁻¹ : plateau interne central

Conditions de Mistral de Nord-Est à 55 km.h⁻¹ : Pointe de l'Espiguette

Conditions de Marin de Sud-Est à 55 km.h⁻¹ : Pointe de l'Espiguette

Conditions de Sud-Ouest à 55 km.h⁻¹ : Pointe de l'Espiguette

Conditions de Tramontane de Nord-Ouest à 55 km.h⁻¹ : Pointe de l'Espiguette

Conditions de Mistral de Nord-Est à 55 km.h⁻¹ : Système Palavasien

Conditions de Marin de Sud-Est à 55 km.h⁻¹ : Système Palavasien

Conditions de Sud-Ouest à 55 km.h⁻¹ : Système Palavasien

Conditions de Tramontane de Nord-Ouest à 55 km.h⁻¹ : Système Palavasien

Conditions de Mistral de Nord-Est à 55 km.h⁻¹ : Secteur des Aresquiers

Conditions de Marin de Sud-Est à 55 km.h⁻¹ : Secteur des Aresquiers

Conditions de Sud-Ouest à 55 km.h⁻¹ : Secteur des Aresquiers

Conditions de Tramontane de Nord-Ouest à 55 km.h⁻¹ : Secteur des Aresquiers

Conditions de Mistral de Nord-Est à 55 km.h⁻¹ : lido à l'Ouest de Sète

Conditions de Marin de Sud-Est à 55 km.h⁻¹ : lido à l'Ouest de Sète

Conditions de Sud-Ouest à 55 km.h⁻¹ : lido à l'Ouest de Sète

Conditions de Tramontane de Nord-Ouest à 55 km.h⁻¹ : lido à l'Ouest de Sète

Short Report - Phase C – Unibo DISTART

Barbara Zanuttigh, Renata Archetti

The general aim of the activities carried out by the research group is the description of the hydro-morphological performance of coastal defence schemes. More specific objectives were

- the analysis of coastal evolution by means of Coastal State Indicators, i.e. significant indicators to be quickly derived in case of great storms;
- the reconstruction of the typical wave climate along the Emilia Romagna littoral and its transfer from deep waters to the shore;
- the analysis of the hydro-morphological response induced by coastal defences by means of 2D numerical modelling;
- the analysis of the real hydro-morphological response induced by coastal defences by means of field surveys (campaigns for wave and current measurements, bathymetric surveys).

To achieve these objectives, two sites were selected along the Emilia-Romagna coast, Lido di Dante (Ra) and Igea Marina (Rm), where the following methodologies were applied:

- analysis of images acquired from the 2 video stations;
- detailed bathymetric surveys;
- field campaign with n.2 Acoustic Doppler Profilers;
- hydro-morphological and hydro-dynamic simulations of the performance of coastal defences by using the 2D numerical code MIKE 21.

Bathymetric surveys

Bathymetric surveys were performed in Lido di Dante

- by ARPA-IA in April 2007 (just before the nourishment), June 2007 (immediately after the nourishment)
- by DISTART in October 2007 (Fig.1).

The analysis of these surveys shows

- a deep erosion hole at the central barrier gap, due to the strong rip current (the crests of both barrier and connectors are placed at m.s.l due to the rock recharge performed in June 2003); this hole bends towards the Southern barrier, presumably due to prevailing of storms from the North, and induces a severe erosion at the barrier toe that may compromise its stability;
- a significant deposition between the Northern barrier and the Northern connector, probably fed by sand transported long-shore and along the groyne from the Northern beach;
- a global tendency to deposition within the protected area, thanks to the sediments transported inshore the barrier by overtopping and to the efficiency of the defence scheme in reducing incident wave energy;
- a deep scour hole of crescentic shape at the Northern barrier roundhead;
- a reduction of the scour hole at the Southern barrier round head, due to the prevailing of Bora events as already documented by the shape of the scour at the central barrier gap.

The extension of the nourishment can obviously be appreciated, and it appears stable at least after six months.

Numerical modelling

Three main tasks were carried out under the 2D numerical modeling with the MIKE 21 suite:

- the reconstruction of the typical near-shore wave climate along the Emilia Romagna littoral, based on existing data from different sources and simulations carried out by ARPA-SIM with SWAN code;
- the evaluation of the hydrodynamic and morphological effects induced by the intervention in Igea Marina, which consisted of lowering 8 emerged barriers and of

laterally confining this area with groynes. The typical climate was reconstructed based on 7 waves with given frequencies and for each wave condition, simulations of waves (PMS module), currents (HD module, see an example in Fig. 2) and sediment transport (ST-Q3);

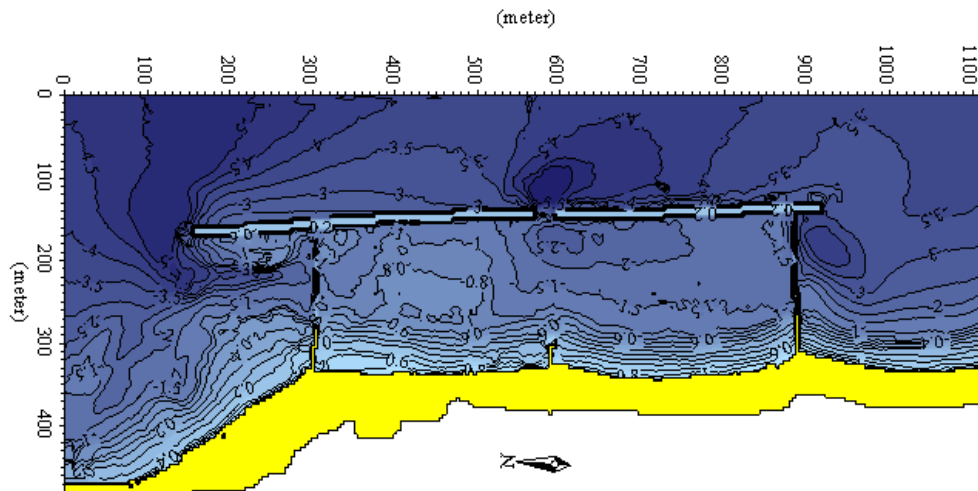


Fig. 1 Multibeam survey in Lido di Dante, October 2007.

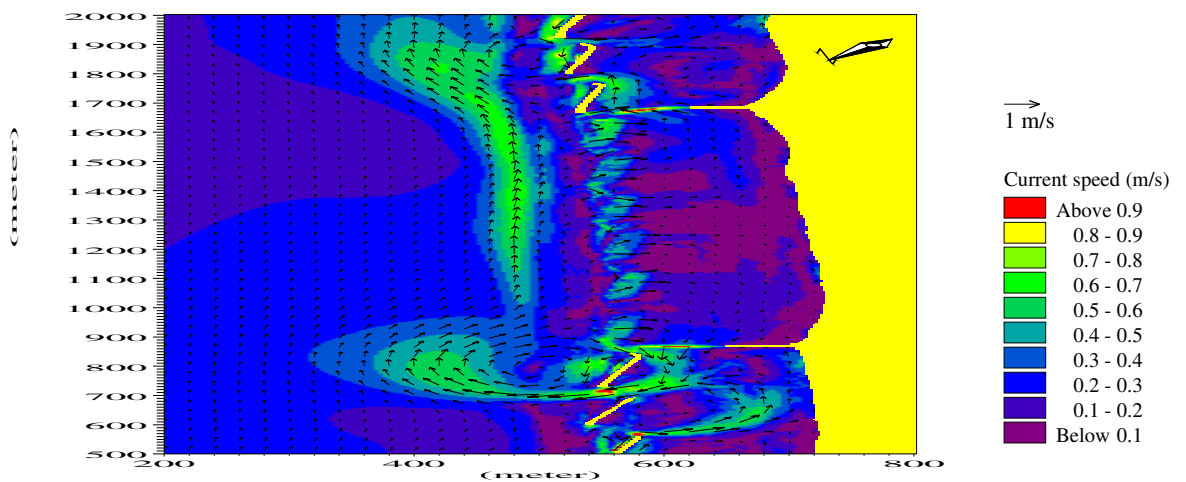


Fig. 2 Current intensities and patterns around the defences of Igea Marina, during a typical Bora event (49° N) with significant wave height $H_s=2.0$ m and average wave period $T_m=8.0$ s m in front of the structures.

- the evaluation of the hydro-morphodynamic response (CAM5 module) induced by the storm after which the two groynes in Igea Marina collapsed. Based on the results of these simulations, the cause of the structural failure of the groynes can be interpreted as the interaction of scour and partial liquefaction. From numerical simulations, high intensity currents occurred at the groyne toes producing a local erosion of about 2.5 m, which is severe but insufficient to induce failure. A partial liquefaction of the groyne foundation may have reduced the soil resistance and induced geotechnical instability. After the failure, the scour hole was found significantly deeper than 2.5 m, probably due to the increase of discharge over the settled groyne. The hole was found partially refilled after the repairing works. This experience proves the importance of a proper design of the structure toe berm in order to contrast local scour, which can be predicted with the support of morphological simulations; of an accurate placement of the geotextile to avoid the migration of fine material; of geotechnical surveys before the works to assess seabed resistance.

Videomonitoring

Collecting data representative of the state of the coastal environment is requisite for successful management of the coastal zone, but a costly and demanding task. Remote sensing techniques have been developed in recent years in order to monitor the beach and the hydrodynamic and morphodynamic processes with success, in particular a technique based on the acquisition and analysis of images was developed since the years '90 by Rob Holman (Holman et al., 1993) that is well known as the ARGUS system. Nowadays about 50 ARGUS stations, developed both for research and coastal management (Aarninkhof et al., 2003; Chickadel and Holman, 2003; Archetti and Lamberti, 2006) have been deployed in the USA, Europe and Australia. Although it is very capable and powerful, for some applications the ARGUS system can be too rigid and expensive.

The analysis of images of a beach is a good candidate which could provide useful information on coastal erosion and recession rates of the shorelines, the location of submerged sandbars and the performance of coastal defence structures. Timex images (long time exposure) offer the possibility to easily detect by eyes and in a semi automatic manner the morphological feature of the coastal environment (shoreline position, bar position etc). Timestacks (high frequency time series of pixel intensities located in appropriate position of the image, Holman et al., 1993) designed perpendicular on the low crested structures and on the beach and parallel close to the structure, allow to detect several important issue of the phenomenon of overtopping, run up, breaking and currents induced by the LCS. These parameters are not easily modelled nor measurable extensively in the field. Two videostations were installed in the Emilia Romagna Region: An ARGUS station was installed in Lido di Dante (Ravenna) in the year 2003 (Albertazzi et al., 2003, Archetti and Lamberti, 2006, Davidson et al., 2007), and a SVM video station was installed in Igea Marina (Rimini) in September 2006 (Archetti et al., in press).

The shoreline position and its evolution in time is a good indicator of the state of the coast (Kroon et al., 2007, Nausicaa Report phase A). At the two studied sites the shoreline position was monitored for the whole period.

In Lido di Dante in 40 months, a total of 72 "video survey" measurements were detected based on video analysis in several transects of the beach. The time series of the shoreline of the protected beach demonstrates a regression tendency equal to about 2.3 m/year.

In Igea Marina the shoreline position was detected with on selected images: good quality images taken during very calm days (and after calm short periods), at the time in correspondence to the sea water level equal to approx. zero. The shoreline was detected on oblique images and then rectified and interpolated in order to have the shoreline position at 1 m spatial resolution.

The evolution of the shoreline can be followed for several sections in figure 3, on the top panel the significant wave height is presented (Hindcasted data by the meteorological service of the Emilia Romagna Region).

The shorelines keeps constant during winter with same small fluctuation of the order of few meters in coincidence with storm events. The behaviour of different sections is comparable, except for section 400 which shows more evident retreat during storms.

Figure 4 shows 3 timestacks used for the hydrodynamic monitoring., The green one is located perpendicular to the structure: it is possible to see the waves breaking on the structure. The red timestack is placed perpendicular to the beach, wave fronts propagating in the direction of the shore and run up are evident. The slope of the breaking is related to the celerity of the waves. In the same figure we can see the timestack given by the array placed perpendicular alongshore the structure (yellow), which allow the estimation of longshore currents.

Timestacks analysis allows to detect run up, wave period, wave direction, frequency of waves overtopping the parallel structures and longshore currents induced by the wave breaking.

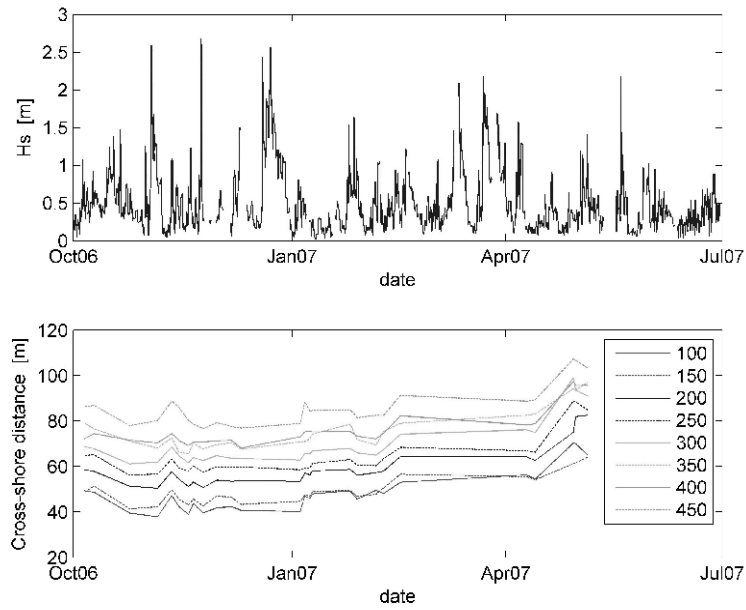


Figure 3. Hs timeseries (top panel), temporal variation of shoreline in 4 beach sections located in Igea Marina (bottom panel). The y axis is given in meters and represents the shoreline migration respect to an arbitrary position. Straight lines in the records correspond to linear interpolation through data gaps. The bold line represent the beginning of the nourishment event in April 2007.

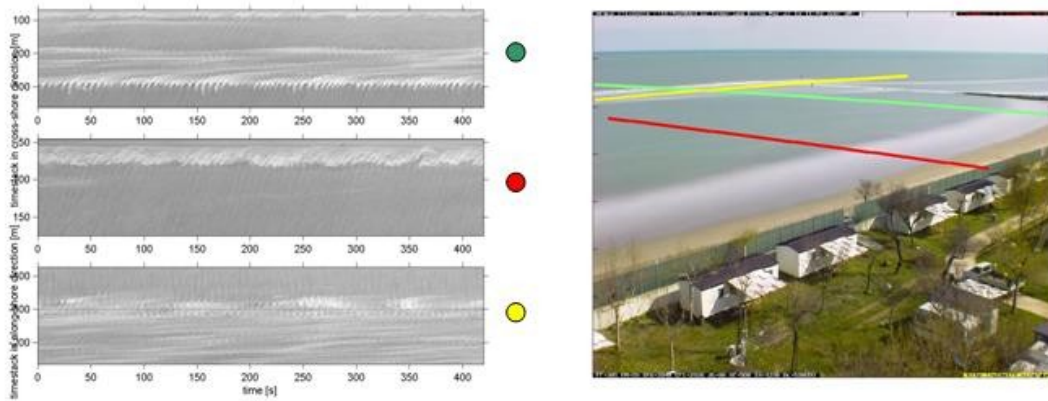


Figure 4: Timestack (high frequency time series of pixel intensities located on the blue array on the image) Lido di Dante, March 22 2007: (Left panel) Timestack located perpendicular to the LCS(green), perpendicular to the beach (red) and alongshore the barrier (yellow). (Right panel) Position of pixel array on the image.

1. INTRODUCTION

In the framework of the NAUSICAA project, the jointed team of the Animal and Human Biology Department of the University of Rome and ISMAR – CNR Venezia, is studying the interactions between coastal erosion, wave climate characterisation and the conditions of the *Posidonia oceanica* beds. In particular, the study aims to understand the role of *P. oceanica* beds in the waves attenuation and in the sediment transport.

This report shortly describes the work due to activities 8, 9 and 10 of the project NAUSICAA. In particular, activities described focused on the implementation of a fully three-dimensional, near-shore ocean circulation model two-way online coupled with a wave model, this in order to carry out simulation of the near-shore dynamics relevant for the region of interest. The simulations carried out include two severe wave storms as well as one ‘typical’ situation. In addition, a fully realistic experiment was performed simulating May 2007 situation, during the period covering the first campaign of *in situ* data collection. All the experiments were carried out including and not including the effect of *Posidonia oceanica* meadows both on waves and current fields.

2. MATERIALS AND METHODS

2.1 The study area

The study area is located in the central Tyrrhenian Sea, between Cape Circeo and the coastal town of Sperlonga (in southern Latium, western Italy) an area corresponding to a coastline 30 km long between latitude $41^{\circ}10'N$ and $41^{\circ}18'N$ and longitude $013^{\circ}05'E$ and $013^{\circ}25'E$ (Fig. 1).

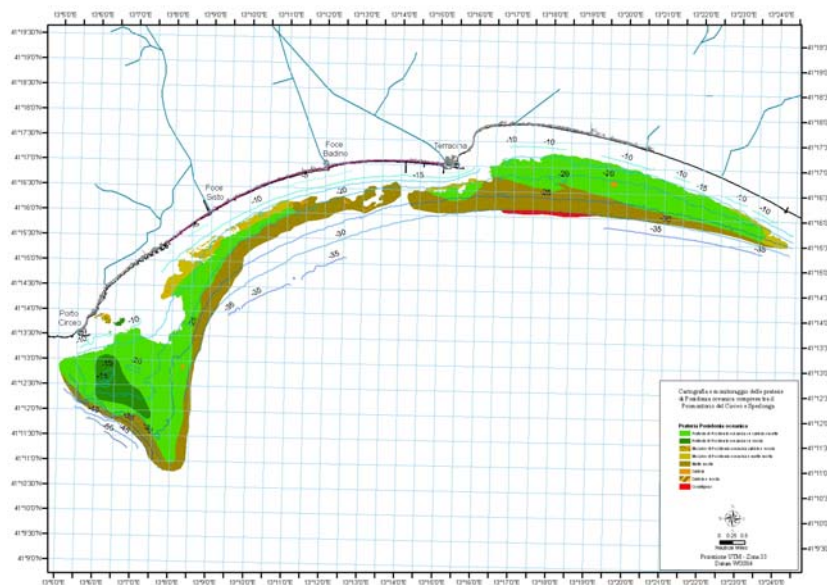


Figure 1 – The study area: west side(upper) and east side (below) of the Circeo – Sperlonga coastline

In the central part of the study area (between Cape Circeo and Terracina), the *P. oceanica* bed shows a heavy regression over time. In 1959, the lower limit of the Posidonia bed was ca 35 m. In the 2005 the lower limit decreased, reaching a depth of 18-20 m. This coast has suffered from significant urban change which has influenced both water quality and sediment type; additionally coastal erosion is very strong. Since 1960 several coast protection works have been carried out.

The eastern area, extending from Terracina to Sperlonga, showed a low-medium regressive status of the Posidonia bed, mainly characterized in a decrease in its lower limits (from 35 m in the 1959 to 25 m in the 2005). The coastline does not display evident signs of erosion.

The upper limit changed less than the lower one, going from 14 m in 1959 to 17-18 m in 2005, without any great diversification in the various sub-areas.

These two sub-areas have been chosen as a “case study” for the NAUSICAA project: the first one as the area with high level of Posidonia beds regression and coastal sedimentation disequilibrium, the second one with the Posidonia bed in good condition and a coastal sedimentation equilibrium.

2.2 *Posidonia oceanica* beds characterization

In the first part of the Nausicaa project (see reports of phase A and B), a cartography of the *Posidonia oceanica* meadows in the study area have been obtained. In the present phase the knowledge on the meadows have been improved to have better information about their conditions.

Structural data concerning the cover and the shoot density of *P. oceanica* were obtained via scuba-diving at depths ranging from 10 to 25 m. Divers recorded key attributes of the meadow, namely: depth, nature of substrate (matte, rock, sand), the features of the meadow, the morphology of the upper or lower limits of the meadow, when encountered. The coverage percentage and the shoots density were also performed. At each site ten shoots of *P. oceanica* were randomly sampled. In laboratory the foliar shoot was separated from the rhizome, then leaves were detached in the order of insertion. Phenological variables were calculated (Buia *et al.*, 2003): mean number of leaves, mean leaf length per shoot, mean width leaves, and Leaf Area Index (mean leaf surface per shoot / 2 x mean shoot density). By means of a GIS software (ArcGis 9.2) the collected data have been utilized to make thematic layers. In particular, map of the *Posidonia oceanica* distribution, map of the Shots Density, map of the Shoots Height, and map of the L.A.I. value have been realized (1:10.000 scale).

2.3 Wave and currents in situ measures

In order to collect water current and waves data, two ADCP (Acoustic Doppler Current Profiler) LinkQuest FlowQuest 600, were deployed on the bottom between S. Felice Circeo and

Terracina). The instruments are able to measure the direction and velocity of the water current along the water column at regularly intervalled time

2.4 Ocean Model ROMS

ROMS (Regional Ocean Modelling System) is a member of a general class of three-dimensional, free surface, terrain following numerical models that solve the Reynolds-Averaged Navier-Stokes equations using the hydrostatic and Boussinesq assumptions. An extensive, in-depth, description of the model can be found in Shchepetkin and McWilliams (2005) or a general description in Haidvogel *et al.* (2000).

2.4.1 Wave Model SWAN

In order to simulate nearshore dynamics, the modification of the momentum equations in ROMS to include the effects of surface waves requires information on the basic wave properties such as wave energy, direction, and wave length. Other processes such as the bottom boundary modules and turbulence closures may additionally require wave periods, bottom orbital velocities, and wave energy dissipation. These wave quantities are currently obtained from the wave model Simulating WAVes Nearshore (SWAN, Booij *et al.*, 1999). SWAN is a phase-averaged model that solves transport equations for wave action density. SWAN accounts for shoaling, refraction, wind-wave generation, wave breaking, bottom dissipation, and nonlinear wave-wave interactions. SWAN also can account for diffraction, partial transmission, and reflection, although not used in this application. Specific formulations for wind input, bottom stress, white-capping, wave-wave interactions are described in detail in Booij *et al.* (2004).

2.4.2 The coupled model ROMS/SWAN

SWAN can be run separately and the output used to force the hydrodynamic and sediment routines (one-way coupling). Alternatively, SWAN can be run concurrently with the circulation model with two-way coupling whereby currents influence the wave field and waves affect the circulation. In this work the two-way coupling has been used. SWAN sends to ROMS arrays of wave height, wave length, wave periods for the water surface and near bed, wave direction, near-bottom orbital velocity, and wave-energy dissipation rate. ROMS provides water depth, sea-surface elevation, and current velocities to SWAN. The exchange of quantities between the models is guaranteed by the coupler Model Coupling Toolkit (MCT). The coupled model ROMS/SWAN also includes a sediment transport module. This model system accounts for all the processes typical of the near-

shore where wave-current interaction are relevant. Full details on the model are provided in Warner *et al.* (2008).

3. IMPLEMENTATION OF *POSIDONIA OCEANICA*

Understanding the effect of the sea grass *Posidonia oceanica* on near-shore dynamics is a challenging area with devoted research basically boosted not before the late 80ies-early 90ies, but even now many processes have not been discerned. Major impacts identified are the reduction of flow speed, the modification of flow and turbulence structure, attenuation of wave energy, thus obviously local modification of sediment transport.

The approaches used up to now are basically two, and both work on tuning the drag coefficient of the bottom friction: Kobayashi-type models and Nepf-type models. The first approach is based on the work of Kobayashi *et al.* (1993), and is focussed on dynamics due to waves only, providing a friction coefficient responsible of wave dissipation based on (wave) Reynolds number. The second approach is based instead only on laboratory experiments with steady flow (no waves), and it is based on the work of Nepf (1999). She assumed that the bottom friction due to seagrass meadows is function of canopy density, and in fact she identified two different regimes with drag coefficient constant (i.e., density-independent) till a certain canopy density threshold and steadily decreasing beyond that value. Very recently, few papers addressed more realistically the issue of modelling seagrass meadows impact on flow-wave-sediment dynamics in the near-shore (e.g. Chen *et al.*, 2007, US Army CEM, 2006). The approach used is basically Nepf-type, and it is focused on the estimate of the bottom drag coefficient for current and, with similar formalism, for waves. The main reason for the choice of this approach is the canopy density range (Nepf results are based on relatively low density range, while Kobayashi very high).

4. BATHYMETRY AND DIGITALIZATION OF *POSIDONIA OCEANICA*

All the simulations performed within the framework of this Research Contract have been carried out using a bathymetry obtained merging data provided by Regione Lazio. The resulting bathymetry is shown in figure 2. The computational grid is divided into 266 x 200 points, with variable resolution (130÷170 m along longitude, 60÷150 m along latitude, with higher resolution in the actual areas covered by *P. oceanica*) and 10 linear terrain following levels on the vertical.

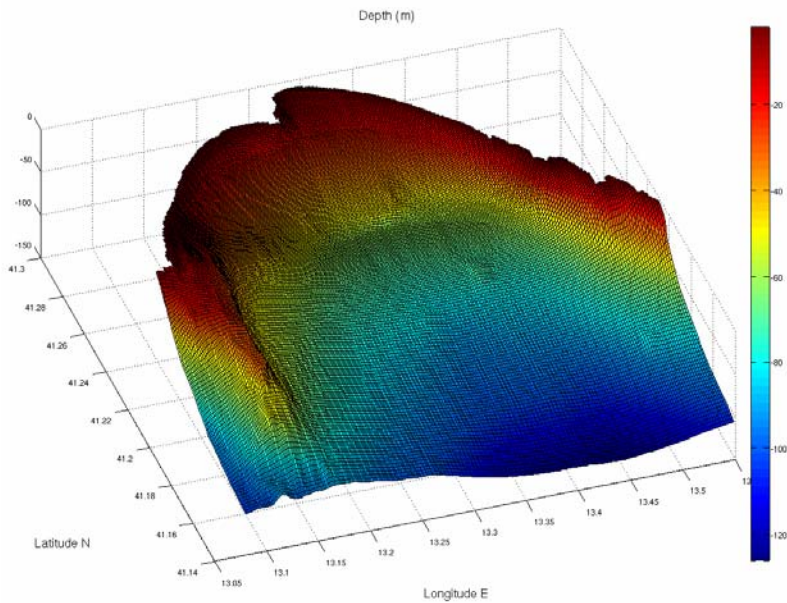


Figure 2 - 3D view of the model bathymetry.

Once the digitalization of the bathymetry was completed, data describing *P. oceanica* meadows geometry and characteristics have been digitalized as well. In figure 3 the white area highlights the area covered by *P. oceanica* as resulted from this process of digitalization.

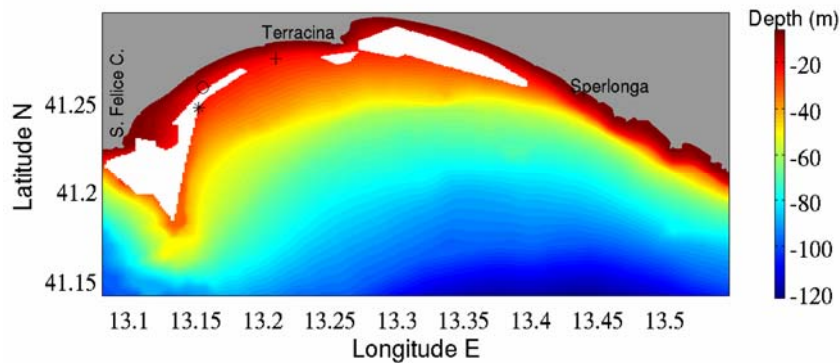


Figure 4 - Model bathymetry (colour scale) and localization of the seagrass meadows (white region) after the digitalization process. The three marks on the figure correspond to the locations of the ADCP during the in situ campaigns of May and June 2007 (“o”, both May and June, “+”, only June, “*”, only May).

According to the numerical modelling of *P. oceanica* presented before, in order to describe the meadows in a realistic way, data on shoot diameter, shoot density and shoot height have been considered. Since the values of these quantities are necessary in each grid cell overlapping the region of the meadows, sparse data collected have been interpolated onto the model grid using standard Objective Analysis procedure. Results are shown in figure 5, 6 and 7.

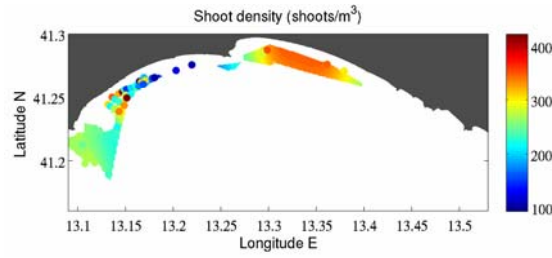


Figure 5 - Shoot density observations (circles) overlapping the field obtained via OA.

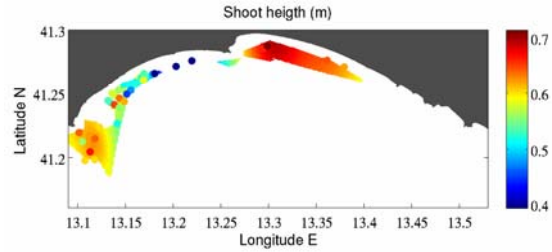


Figure 6 - Shoot height observations (circles) overlapping the field obtained via OA.

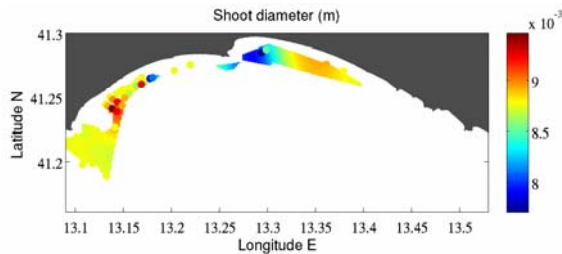


Figure 7 - Shoot diameter observations (circles) overlapping the field obtained via OA.

5. SIMULATION OF THE NEARSHORE DYNAMICS: THE ‘CLIMATOLOGICAL’ CASES

The coupled system ROMS/SWAN was run in two different extreme event scenarios and one ‘average’ scenario. These scenarios were identified on the basis of the offshore wave climate analysis carried out in the Phase A and B of this project. The direction of provenance of extremely severe climate conditions are west, south-west and south-east. When transferring the offshore wave conditions to the coast, it was observed that directions from west either don’t hit the coastline in the Gulf or are turned to a more south-west incident direction. For this reason, severe wave storms coming from the sector $250^{\circ} \div 280^{\circ}$ are not considered here.

Instead, south-west and south-east directions are considered. These directions also highlight a possible different response of the two sample regions to different forcing. Then, as said, also a “typical” wave field was considered, i.e., the median in the combined sample distribution of directions and significant wave height. In this case, the median has been estimated on a sub-set of whole sample; in fact, all cases with significant wave height lower than 0.5 or directions non relevant for the Gulf (from West, North, East) have not been considered.

Each of these three simulations was run with and without *P. oceanica* implemented in two different ways; therefore, for a total of 9 numerical experiments that are conveniently summarised in Table 1.

	TEST 1	TEST 2	TEST 3
Hsig (m)	5.25	5.25	1.00
T01 (s)	9.5	10.0	6.0
Wave Dir (°N)	145	225	215
Wind Speed (m/s)	10	10	5
Wind Dir (°N)	145	225	215
<i>Without Posidonia oceanica</i>			
	TEST 4	TEST 5	TEST 6
Hsig (m)	5.25	5.25	1.00
T01 (s)	9.5	10.0	6.0
Wave Dir (°N)	145	225	215
Wind Speed (m/s)	10	10	5
Wind Dir (°N)	145	225	215
<i>With Posidonia oceanica following Chen et al., 2007</i>			
	TEST 7	TEST 8	TEST 9
Hsig (m)	5.25	5.25	1.00
T01 (s)	9.5	10.0	6.0
Wave Dir (°N)	145	225	215
Wind Speed (m/s)	10	10	5
Wind Dir (°N)	145	225	215
<i>With Posidonia oceanica using ISMAR wave friction factor and Chen et al., 2007 drag coefficient for current</i>			

Table 1. Configuration of the ‘climatological’ experiments. Hsig is the significant wave height, T01 the mean period, Wave (Wind) Dir the direction of provenance of the wave (wind) field.

5.1 Intercomparison of test 3 – Test 6 – Test 9 application

As example of the elaboration carried out, we report the intercomparison of test 3 – 6 and 9 application. Three tests were performed for the ‘typical’ wave field from south-west, without *P. oceanica* (Test 3, “control run”), with the effect of *P. oceanica* implementing its effect following Chen *et al.*, 2007 (Test 6) and using Chen *et al.*, 2007 for the current drag coefficient and ISMAR friction factor (Test 9). The results of the bottom current field can be seen in fig. 8, with major current speed decrease in correspondence of the locations of the meadows, in particular in the western sector. It should be kept in mind however, that the magnitude of bottom currents in this scenario is really low, and it can be reasonably overwhelmed by the large scale circulation. Wave fields from the three cases are shown in fig. 9, with only minor differences due to the lower wave field less interacting with the bottom. The integrated effect of the circulation and wave field on sediment transport can be seen in fig. 10, although. What is clear again, even in such ‘typical’ and not ‘extreme’ given wave field, is that, as in the previous experiments, downwind the meadows sediment erosion/deposition is weaker.

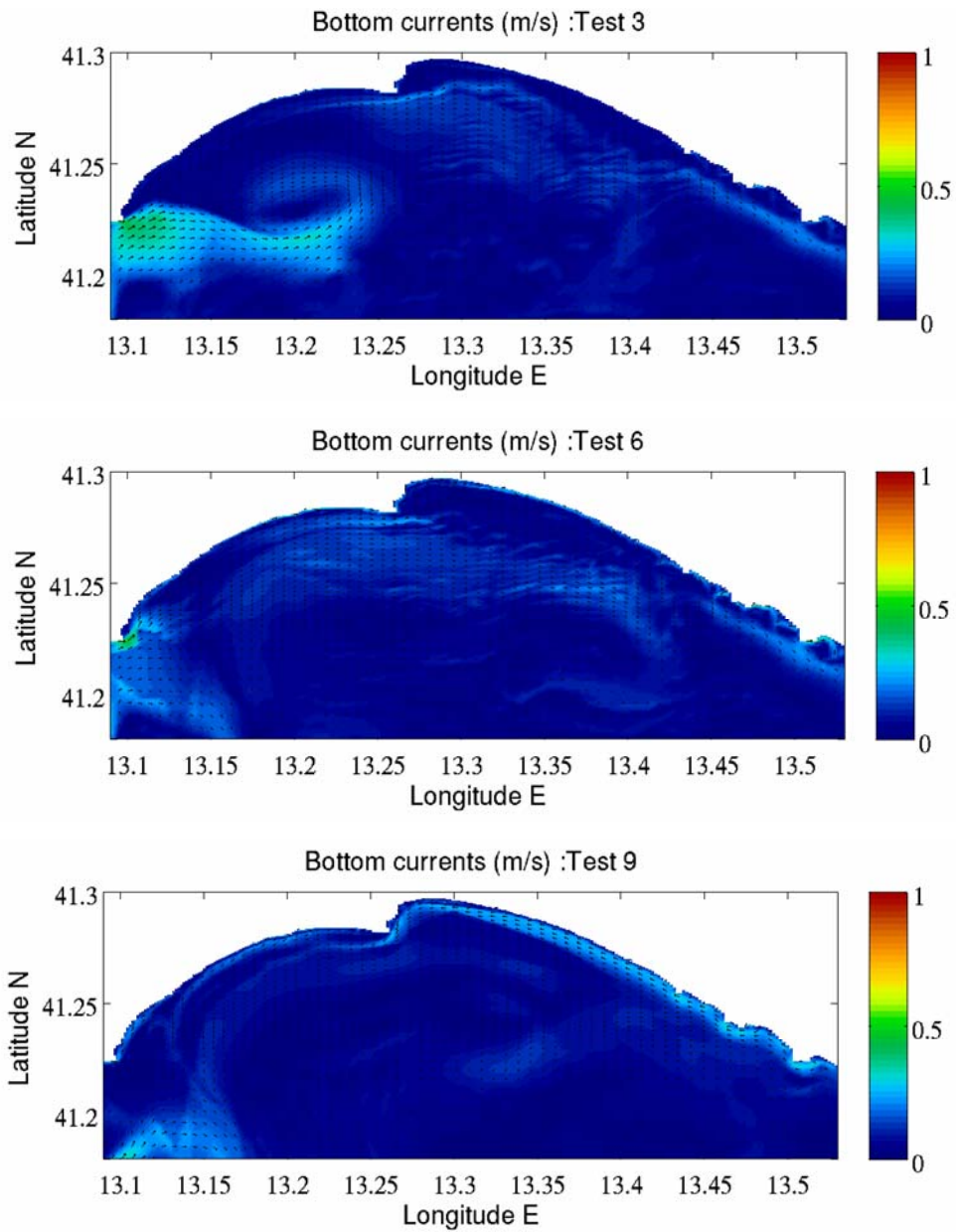


Figure 8 - Bottom current difference after 3 days of simulation from experiment T6 - T3 (upper panel) and T9 - T3 (lower). The difference is plotted for enhance readability. It can be noticed that area of effect of the meadows are associated to major current decreases (blue colour).

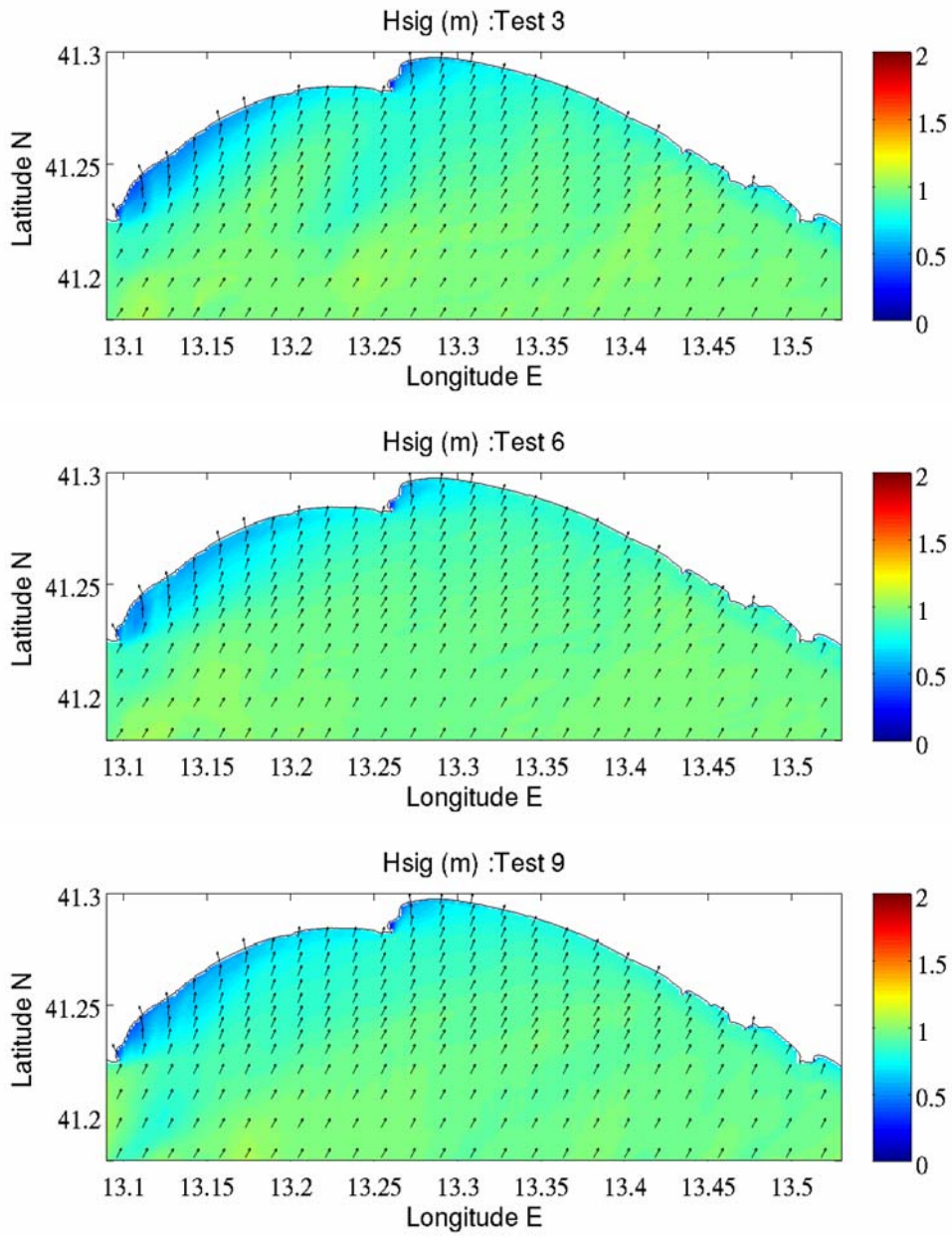


Figure 9 - Significant wave height after 3 days of simulation from experiment T3 (upper panel), T6 (middle) and T9 (lower).

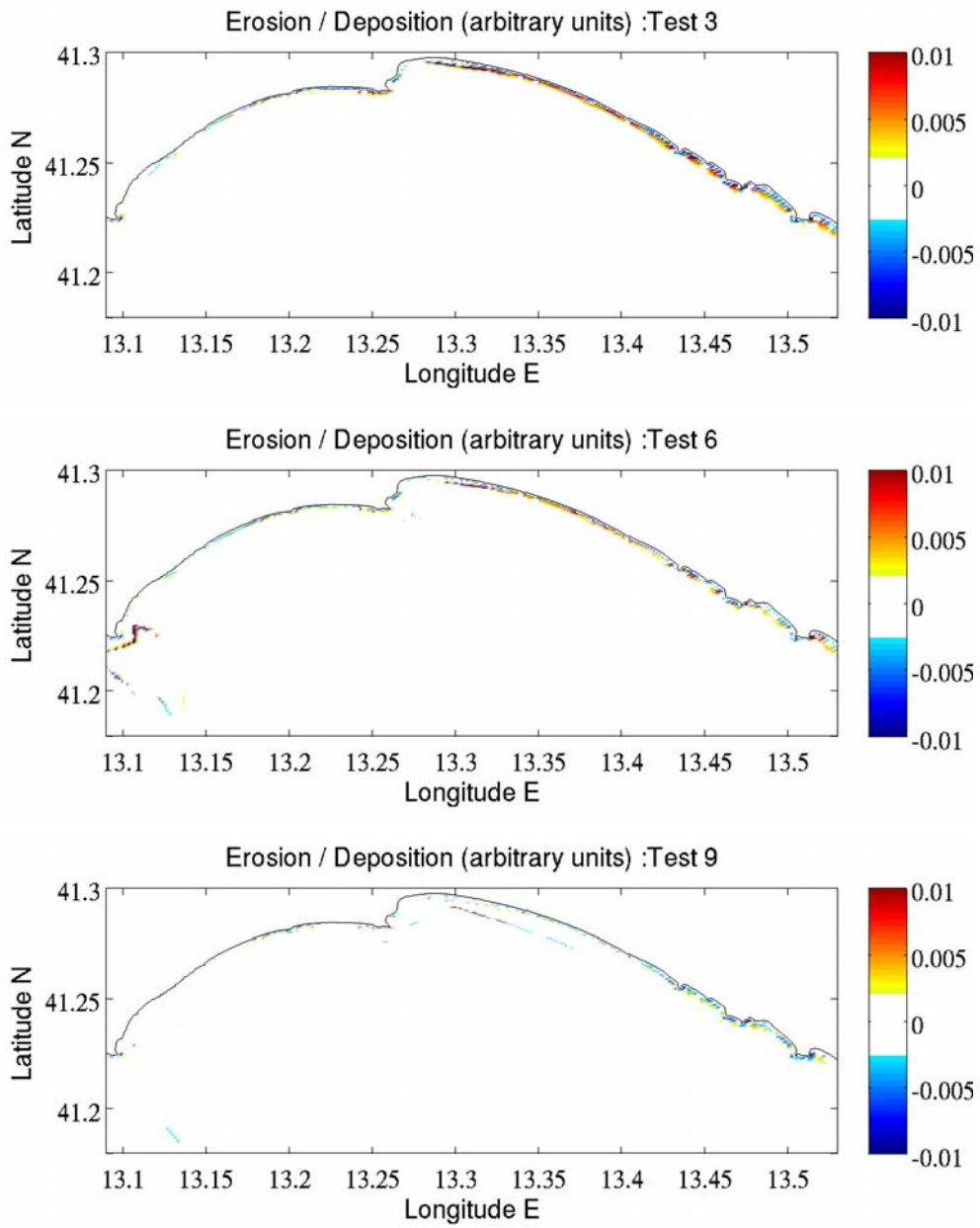
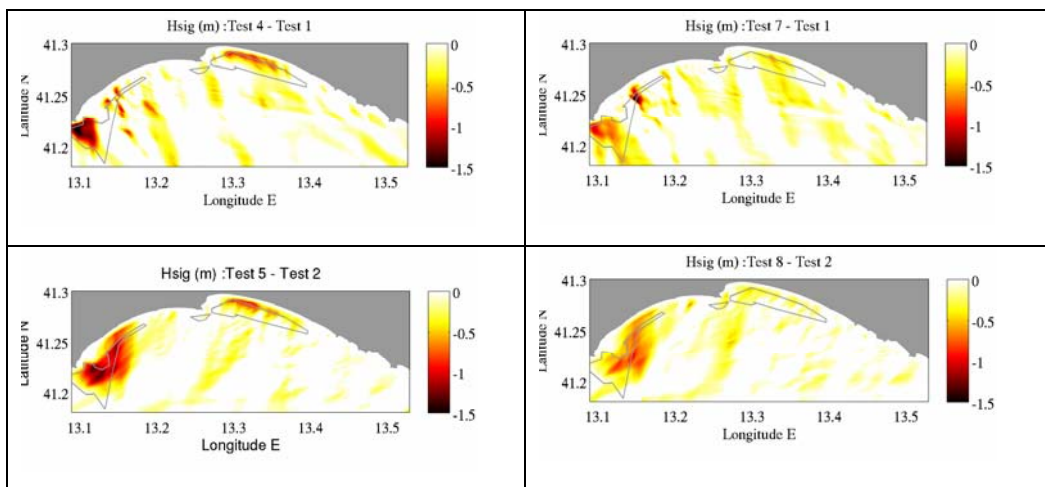


Figure 10 - Erosion/deposition index after 3 days of simulation from experiment T3 (upper panel), T6 (middle) and T9 (lower). This index is expressed in arbitrary unit and it is a measure of the tendency of erosion or deposition.

5.2 Intercomparison of wave dissipation associated to incoming direction of the wave storm

A direct comparison between the wave field reduction associated to the effect of the seagrass is presented in figure 11. It can be noticed that the use of the wave friction factor following Chen *et al.* (2007) (left panel of the figure) gives more dissipation compared to ISMAR friction factor (right panel). However, in Test 5 and Test 8 vs. Test 2 the reduction in wave height is larger compared to Test 4 and 7 vs. Test1. This is associated to the relative role played by the direction of provenance of the wave storm and the location of the meadows. *P. oceanica* seems to affect the wave field in the Gulf in particular when the wave storm comes from the south-west. Note that the reduction can be as large as 1.5 m , which is roughly 30-40 % of the wave height in the control run.



Figure

11 -

Difference in significant wave height amongst the tests with severe wave storm (upper panel, coming from SE; lower panel coming from SW).

7. THE REALISTIC EXPERIMENT

ROMS/SWAN coupled model was run also in a fully realistic configuration, in order to simulate the period 11-19 May 2007 overlapping the first phase of *in situ* data during the project. This experiment is due as a test of feasibility of simulation of the real near-shore circulation and not only idealized, climatological test cases. In this case, a total of three experiments have been carried out: TEST A: without *P. oceanica* (control run); TEST B: with *P. oceanica* implemented following Chen *et al.*, 2007 for both current drag and wave friction factor; TEST C: with *P. oceanica* implemented following Chen *et al.*, 2007 for current drag and using ISMAR wave friction factor. Current data coming from the run with ROMS/SWAN was compared to the data collected *in situ* in the location shown in figure 3. Current data from the ADCP measurements have been extracted, filtered in order to remove the tidal signal and integrated along the water column in order to have a de-tided time series of depth integrated currents every 30 minutes. These currents are compared to the corresponding model output every 30 minutes. Results are shown in figure 14 (ADCP location

more close to the shore) and figure 15 (ADCP location offshore). In the figure 12 and 13 are shown four panel, that is, measurements and the results from the three numerical experiment. It can be noticed that the circulation is generally variable, with an average anticyclonic circulation in the first part of the time series (till 15 May) and than a reverse to a cyclonic circulation. The comparison model-observations shows some discrepancies in the very first part and very last part of the period, while in the period 13-17 May the model is generally able to resemble observations, with however some differences amongst the numerical experiments.

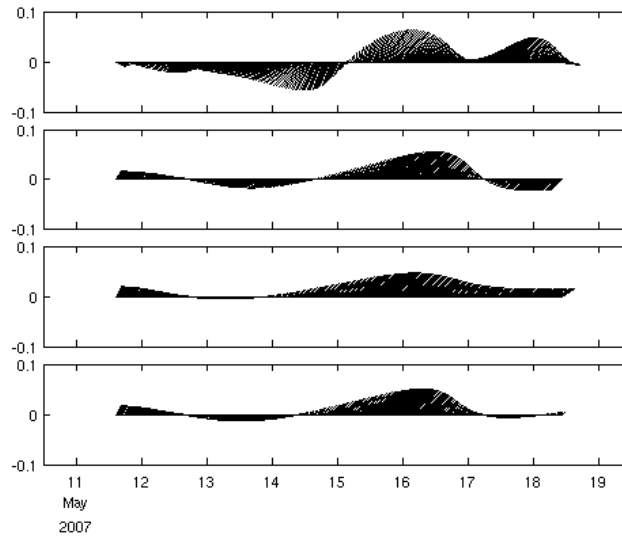


Figure 12 - Comparison of de-tided depth integrated current measured with the ADCP (top panel), from model output Test A (second panel from top), from model output Test B (third panel from top), from model output Test C (bottom panel), at the inshore location. Units are m/s.

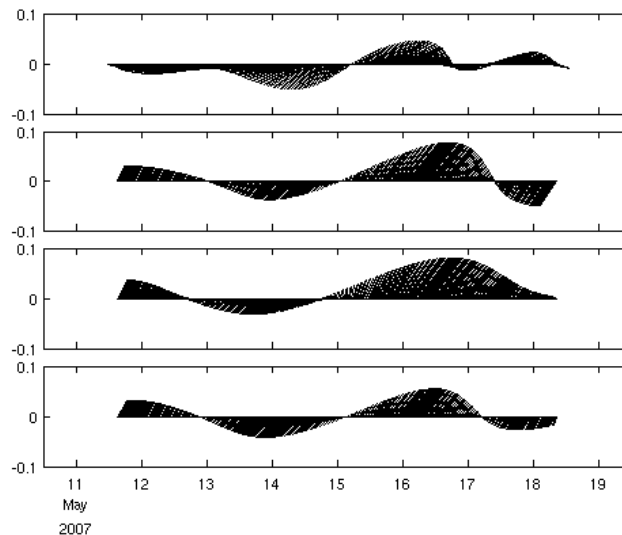


Figure 13 - Comparison of de-tided depth integrated current measured with the ADCP (top panel), from model output Test A (second panel from top), from model output Test B (third panel from top), from model output Test C (bottom panel), at the offshore location. Units are m/s.

In order to evaluate the performance of the different model experiments versus the observations, a complex correlation score was evaluated. This score gives a measure of the co-variance over time of the modelled vs. observed time series and also possible differences in the dominant direction. This score can be used to understand in a statistical approach the performance of the numerical experiments. Correlations are generally fair, and Test B gives better value, suggesting a better agreement with the observations in time variability of the currents. The comparison with the offshore ADCP is much better than the comparison with “inshore” ADCP, while in the other two experiments the difference is not so noticeable. Discrepancy in the main direction (complex part of the correlation) suggests that the models (irrespective case A, B, or C) are generally aligned with the “inshore” ADCP current field, while there is a 25-30° offset counterclockwise compared to the “offshore” ADCP current field.

In statistical sense, it can be stated that experiment B is performing better, even if the alignment with observations is a few degrees lower compared to test A and C.

7. CONCLUDING REMARKS

This report outlines the activity of the Animal and Human Biology Department of Rome University and the Institute of Marine Sciences of the Italian National Research Council, activity devoted to simulate the near-shore dynamics of the Gulf of Terracina by means of numerical experiments. The near-shore dynamics is reconstructed using the full three dimensional coupled model ROMS/SWAN. The effect on the circulation of *Posidonia oceanica* was implemented in the model following the recent literature on the subject and using observations collected in situ featuring the meadows characteristics (shoot density, shoot height, shoot diameter). In order to understand the dynamics of the region of interest, 3 different “wave storms” were simulated, whether including or not the effect of the seagrass meadows. These three “wave storms” have been selected based on the offshore wave analysis and include the two most severe storms attacking the Gulf of Terracina and a “typical”, definitely less energetic, wave field. From these experiments it was outlined that *Posidonia oceanica* seems to protect the area downwind, since the sediment mobilization along the shoreline was found to be lower. This means, for example for a wave storm from south east, that the western part of the gulf is protected by the presence of *Posidonia oceanica*, in other words the energy attacking the shore is lower. For the wave storm coming from the south-west, the effect of *Posidonia oceanica* is even larger, because the meadows (and the shallow region to the south of San Felice Circeo) definitely impact on the incoming wave storm, so lesser mobilization of sediment is found not only in the eastern part of the gulf, while also in the western. Even in the ‘typical’ low energy scenario, *Posidonia oceanica* was found to reduce sediment mobilization down-current, of

course to a lower extent. Careful has to be used when interpreting the sediment index. The close proximity between the area of deposition and the area of erosion alongshore seems to be associated to a formation of sand structures like bars. This is probably due to the fact that model bathymetry has been considered as a “flat” slope, but at the dynamical equilibrium, the model tends to develop some large ripples which are not resolved by the bathymetric dataset. In addition, the sediment erosion/deposition index has to be considered strictly associated to the storm producing it, and not to an “average” situation.

The fully realistic experiments simulating the period 11-18 May 2007 was carried out as a proxy for future similar experiments. Even if in this case some features of the circulations of the area have been neglected (i.e., the large scale circulation was not provided at the boundary, tides are simulated only as M2 neglecting other components, temperature and salinity for the initialization are climatological and not observed in situ), these experiments were successfully performed and the comparison with observations suggested a good agreement with the available observations. Therefore, it can be concluded that ROMS/SWAN is an useful tool that can help the understanding of the near-shore dynamics in the region with acceptable confidence on the results.

8. REFERENCES

- Booij N., Ris R. C., and Holthuijsen, L. H., (1999) - A third-generation wave model for coastal regions, Part I, Model description and validation, *J. Geoph. Research*, 104, C4. 7649-7666.
- Booij, N., Haagsma, I.J.G., Holthuijsen, L.H., Kieftenburg, A.T., Ris, R.C., Van der Westhuysen, A.J., and Zijlema, M. (2004) - SWAN Cycle III version 40.41 User Manual, Delft University of Technology.
- Buia M.C., Gambi M.C. Dappiano M., (2003) - I sistemi a fanerogame marine. *Biol. Mar. Medit.*, 10: 145-198.
- Chen S. N., Sanford L. P., Koch E. W., Shi F. and North E. W., (2007) - A nearshore model to investigate the effects of seagrass bed geometry on wave attenuation and suspended sediment transport. *Estuaries and Coasts*, 30: 296-310.
- Haidvogel, D. B., Arango, H. G., Hedstrom, K., Beckmann, A., Malanotte-Rizzoli, P., and Shchepetkin, A. F., (2000) - Model evaluation experiments in the North Atlantic Basin: Simulations in nonlinear terrain-following coordinates. *Dynamics of Atmospheres and Oceans*, 32: 239-281.
- Kobayashi, N., Raichle A. W. and Asano T. , (1993) - Wave attenuation by vegetation. *Journal of Waterway Port Coastal and Oceanic Engineering-ASCE*, 119: 30-48.
- Nepf, H. M., (1999) - Drag, turbulence and diffusion in flow through emergent vegetation. *Water Resources Research*, 35: 479-489.
- Shchepetkin, A., J. C. McWilliams, (1998) - Quasi-monotone advection schemes based on explicit locally adaptive dissipation. *Monthly Weather Review*, 126: 1541-1580.
- U.S. Army Corps of Engineers, (2002) - Coastal Engineering Manual. Engineer manual 1110-2-1100, US Army Corps of Engineers, Washington, D. C.
- Warner, J. C., Sherwood, C. R., Signell R. P., Harris C. H. and Arango H. G., (2008) - Development of a three dimensional, regional, coupled wave, current and sediment transport model. *Computational Geoscience*, in press.